

1 **A COMPARISON OF SATELLITE DATA-BASED DROUGHT INDICATORS IN**
2 **DETECTING THE 2012 DROUGHT IN THE SOUTHEASTERN US**

3 *Ali Levent Yagci^a, Joseph A. Santanello^a, Matthew Rodell^a, Meixia Deng^b,*
4 *Liping Di^b*

6 *^a NASA Goddard Space Flight Center, Hydrological Sciences Lab. (617),*
7 *Greenbelt, MD 20771, USA*

8 *^b George Mason University, Center For Spatial Information Science and*
9 *Systems, Fairfax, VA 22030, USA*

10

11 **Abstract**

12 The drought of 2012 in the North America devastated agricultural crops and pastures, further
13 damaging agriculture and livestock industries and leading to great losses in the economy. The
14 drought maps of the United States Drought Monitor (USDM) and various drought monitoring
15 techniques based on the data collected by the satellites orbiting in space such as the Gravity
16 Recovery and Climate Experiment (GRACE) and the Moderate Resolution Imaging
17 Spectroradiometer (MODIS) are inter-compared during the 2012 drought conditions in the
18 southeastern United States. The results indicated that spatial extent of drought reported by
19 USDM were in general agreement with those reported by the MODIS-based drought maps.
20 GRACE-based drought maps suggested that the southeastern US experienced widespread decline
21 in surface and root-zone soil moisture and groundwater resources. Disagreements among all
22 drought indicators were observed over irrigated areas, especially in Lower Mississippi region
23 where agriculture is mainly irrigated. Besides, we demonstrated that time lag of vegetation
24 response to changes in soil moisture and groundwater partly contributed to these
25 disagreements, as well.

26

27 **Keywords:** Drought monitoring; Drought indicators; MODIS; GRACE; USDM.

28 1. Introduction

29 Drought is one of the devastating natural hazards, which often recurs when plants cannot
30 sustain their growth as a result of water deficit. Its occurrence interferes with agricultural
31 production by significantly reducing crop yields, in turn damaging the global economy. As the
32 world population has been steadily growing, food supply must keep up with this increasing
33 demand.

34 In this regard, several drought monitoring tools such as United States Drought Monitor
35 (USDM) (Svoboda et al. 2002) and Global Agricultural Drought Monitoring and Forecasting
36 System (GADMFS) (Deng et al. 2013) have been developed to detect onset, duration, extent and
37 severity of drought and timely inform state and government agencies, stake-holders, farmers and
38 public so that its devastating effects can be mitigated.

39 Observations obtained by satellites orbiting in space are indispensable to routinely track the
40 Earth's ground and surface water resources and natural hazards such as droughts and floods, etc.
41 In the last decade, many efforts have been devoted to drought monitoring. Drought is relatively
42 defined natural phenomenon, generally identified by the deviations of precipitation (e.g.,
43 meteorological drought), soil water (e.g., agricultural drought) and ground water and streamflow
44 (e.g., hydrological drought) from their long-term average condition (Wilhite 2000).

45 Remotely-sensed vegetation indices such as the Normalized Difference Vegetation Index
46 (NDVI) have been extensively used to track droughts (Kogan 2001), especially from the NOAA's
47 Advanced Very High Resolution Radiometer (AVHRR) because of its long record (e.g., ≈ 30 years).
48 Vegetation indices are good surrogate measures of photosynthetically functioning vegetation

49 (Tucker and Choudhury 1987). Because drought hinders the photosynthetic activity of plants,
50 large-scale reduction in NDVI over a region (e.g., statewide) can be associated with droughts.
51 After completing the 10 years in orbit, the products of NASA's Moderate Resolution Imaging
52 Spectroradiometer (MODIS) have been also used to monitor droughts (Yagci et al. 2012; Deng et
53 al. 2013). MODIS acquires observations in narrower bands than the AVHRR instrument,
54 successfully avoiding the water vapor absorption in the Visible-RED (RED) and Near-Infrared (NIR)
55 region of the electromagnetic spectrum. Therefore, MODIS-NDVI products attain relatively larger
56 values and better accuracy in exhibiting temporal profiles of forests than the AVHRR-NDVI data
57 (Huete et al. 2002).

58 In addition to NDVI, ability of surface brightness temperature (T_b) or land surface
59 temperature (LST) to track drought has been successfully tested and validated against the crop
60 yields in the state of Texas, U.S.A (Yagci et al. 2011) and around the globe (Kogan 2001). LST is
61 better indicator of surface temperature conditions than T_b since it is corrected for surface
62 emissivity and estimated from surface radiance, i.e., atmospherically corrected surface radiance
63 reaching the sensor. LST is a proxy for moisture availability and evapotranspiration conditions
64 such that water depletion in the plant root zone leads to stomatal closure, reduced transpiration
65 and subsequently elevated canopy temperatures (Anderson and Kustas 2008). Drought detected
66 by NDVI and LST products is referred to as vegetative drought or agricultural drought.

67 In recent years, a new way has surfaced to monitor drought through analysis of the terrestrial
68 water storage (TWS) anomalies. The monthly variations in the Earth's gravitational signal
69 measured by twin satellites of the Gravity Recovery and Climate Experiment (GRACE) have been
70 shown to relate to monthly TWS changes with roughly 1.5 cm accuracy at regional scales (Wahr

71 et al. 2004). GRACE-derived TWS is coarsely resolved and contains vertically-integrated
72 information about surface and sub-surface water conditions, therefore its spatial, temporal, and
73 vertical decomposition into soil moisture and groundwater components achieved through data
74 assimilation into the Catchment Land Surface Model (CLSM) aids in its interpretation and
75 application to drought monitoring (Houborg et al. 2012; Rodell 2012). The resulting groundwater
76 and soil moisture wetness fields are appropriate for hydrological and agricultural drought
77 monitoring applications, respectively.

78 USDM is a collaborative effort by the National Drought Mitigation Center of the University
79 of Nebraska—Lincoln, the Departments of Commerce and Agriculture and outside experts to
80 summarize weekly drought conditions across the U.S. (Svoboda et al. 2002). Despite the fact that
81 USDM is the premier drought product for the U.S., it does have certain shortcomings such as a
82 tendency towards overestimation of drought areal coverage and difficulty in representing the
83 local-scale (e.g., county-scale) conditions, which have been highlighted by several studies (Brown
84 et al. 2008; Tadesse, Brown, and Hayes 2005).

85 The conterminous U.S. experienced a vast costly drought in 2012 which caused disastrous
86 impacts on agriculture and livestock industries, totaling nearly \$30 billion losses (Rippey 2015).
87 The drought of 2012 was similar to the drought of 1988 in terms of cost and the mega-drought
88 of the 1950s in terms of areal coverage (Rippey 2015). In this study, characteristics of the 2012
89 drought are examined using the drought maps derived from the aforementioned approaches.
90 Each method is rather distinct in terms of input type and source, theoretical background and level
91 of complexity. Their results are inter-compared in 2012, and their similarities and discrepancies
92 are also highlighted in Southeast US.

93 **2. Data and Methods**

94 **2.1. NDVI**

95 NDVI is a measure of vegetation greenness, ranging from -1 to 1. Presence of chlorophyll
96 pigments in plant leaves causes visible sunlight in RED region of the spectrum to be absorbed for
97 photosynthesis and sunlight in NIR region of spectrum is substantially reflected due to cell
98 structure of the leaves. Therefore, green healthy functioning vegetation, always attains larger
99 NDVI value than brown stressed vegetation. Swain et al. (2011) demonstrated that NDVI in the
100 drought year of 2002 was considerably smaller than NDVI during the non-drought year, 2007
101 over the croplands and grasslands of Nebraska, U.S. The 16-day composite MODIS-NDVI products
102 (Collection 5) were retrieved from the NASA's Land Processes Distributed Active Archive Center
103 (LP DAAC). The level-3 NDVI products, abbreviated as MOD13A2.005, are compiled from
104 radiometrically-, geometrically- and atmospherically-corrected surface reflectances and have 1-
105 km spatial resolution. The compositing algorithm, the constrained view angle maximum value
106 composite (CV-MVC), picks the best available NDVI observation that is non-cloudy and closest to
107 nadir view to represent the vegetation conditions during the 16-day period (Solano et al. 2010).

108 **2.2. LST**

109 LST is a proxy variable for moisture availability and evapotranspiration conditions (Anderson
110 and Kustas 2008). Elevated LSTs are typical during drought years as opposed to LSTs observed in
111 normal or wet years since plants are not transpiring to cool off the canopy. Likewise, Swain et al.
112 (2011) demonstrated that LST increased during the 2002 drought year in comparison to the 2007
113 normal year in the croplands (corn) and grasslands of Nebraska. The collection 5 daytime MODIS-

114 LST products were retrieved from the NASA's LP DAAC. The level-3 LST products, abbreviated as
115 MYD11A2.005, are composited over a 8-day period with 1-km spatial resolution and calculated
116 from radiometrically-, geometrically- and atmospherically-corrected surface radiances. Unlike
117 16-day NDVI composites, the 8-day LST composite is the average of all non-cloudy LSTs during
118 the 8-day period (Wan 2007).

119 **2.3. Vegetation Condition Index (VCI)**

120 The Vegetation Condition Index (VCI) was introduced to separate the annually varying NDVI
121 component due to prevailing weather conditions from long-term component of NDVI (e.g.,
122 climate, soil and land cover type) (Kogan 1997). The index ranges from 0 to 100 and can be
123 calculated with the following formula:

$$VCI_c = 100 \times \frac{NDVI_c - NDVI_{min}}{NDVI_{max} - NDVI_{min}} \quad (1)$$

124 where $NDVI_{min}$ and $NDVI_{max}$ are the multi-year minimum and maximum NDVI values,
125 respectively, and $NDVI_c$ is the NDVI value of the compositing period of interest. For instance, if
126 VCI of the 177th day of 2012 is the interest, then $NDVI_c$ is the NDVI value of the 177th day of
127 2012. VCI values of 0 and 100 indicate the worst and best vegetation conditions, respectively.
128 Prior to VCI calculation, low-quality NDVI pixels that are covered with cloud, cloud shadows and
129 adjacent to clouds were removed based on quality flags in the corresponding quality assurance
130 (QA) layers that come with the NDVI products. The resulting gaps in NDVI products were filled by
131 interpolation. NDVI observations from two preceding and following 16-day periods along with
132 their corresponding day of year (DOY) information were used to interpolate gaps and downscale

133 to 8-day temporal resolution. The VCI-based drought maps were compiled by the percentile-
134 based classification scheme given in Table 1.

135 **2.4. Temperature Condition Index (TCI)**

136 Similar to VCI, TCI was designed to highlight LST changes due to prevailing weather conditions
137 (Kogan 1997). It ranges from 0 to 100 and can be calculated with the following formula:

$$TCI_c = 100 \times \frac{LST_{max} - LST_c}{LST_{max} - LST_{min}} \quad (2)$$

138 where LST_{min} and LST_{max} are the multi-year minimum and maximum LST values, respectively,
139 and LST_c is the LST value of the compositing period of interest. For instance, if TCI of the 177th
140 day of 2012 is the interest, then LST_c is the LST value of the 177th day of 2012. Minimum and
141 maximum TCI values (e.g., 0 and 100) indicate the worst and best vegetation conditions,
142 respectively. Prior to TCI calculation, LST products underwent a masking process where all cloudy
143 LST observations were removed. The incomplete LST time series were filled by temporal
144 interpolating using LST observations from two preceding and following 8-day compositing
145 periods. The TCI-based drought maps were categorized by the drought classification scheme in
146 Table 1 to identify drought-affected areas.

147 **2.5. United States Drought Monitor (USDM)**

148 The team of roughly 15 authors of the USDM combines meteorological, agricultural and
149 hydrological drought indicators such as Palmer Drought Severity Index (PDSI), Climate Prediction
150 Center (CPC) soil moisture model, US Geological Survey (USGS) weekly streamflow, Standardized
151 Precipitation Index (SPI) and other drought indices to produce weekly drought maps, by focusing

152 on broad-scale conditions (e.g., state-level). In turn, it may not be used to infer local-scale (e.g.,
 153 county-level) conditions. Drought is classified by percentiles into 5 different severities,
 154 abnormally dry, moderate, severe, extreme and exceptional drought, as outlined in Table 1 (The
 155 National Drought Mitigation Center 2016). In the end, a blend of drought indicators with different
 156 weights determined subjectively by the experts contributes to the final drought map (Svoboda
 157 et al. 2002), and this map is updated weekly and disseminated via the USDM website
 158 (<http://droughtmonitor.unl.edu/Home.aspx>).

159

Table 1 - USDM Drought Classification Scheme

Category	Description	Percentiles
D0	Abnormally Dry	21 to 30
D1	Moderate Drought	11 to 20
D2	Severe Drought	6 to 10
D3	Extreme Drought	3 to 5
D4	Exceptional Drought	0 to 2

160 **2.6. GRACE-based Drought indicators**

161 Earth's gravity field varies in space and time as a result of heterogeneities and movements of
 162 mass at the surface, including redistribution of terrestrial water storage (TWS). GRACE detects
 163 these gravitational variations as they perturb the orbits of its twin satellites (Tapley et al. 2004;
 164 Wahr et al. 2004), and uses them to infer monthly changes in TWS at regional scales (>150,000
 165 km²) (Swenson et al. 2006). In addition to its coarse spatial and temporal resolutions, GRACE
 166 alone cannot separate changes in groundwater, soil moisture, surface waters, and snow/ice
 167 (Rodell and Famiglietti 1999). Zaitchik, Rodell, and Reichle (2008) proposed a data assimilation

168 method based on the Catchment Land Surface Model (Koster et al. 2000) to downscale and
169 vertically decompose GRACE-based TWS. Later, Houborg et al. (2012) applied this data
170 assimilation approach to GRACE-derived TWS and produced drought indicators for surface soil
171 moisture (SFSM), root-zone soil moisture (RTSM) and ground water storage (GWS) in 0.125
172 degree resolution, which conformed to the percentile ranges proposed by the USDM (Table 1),
173 thus delineating drought-affected areas across the continental U.S.. SFSM and RTSM are
174 indicative of agricultural drought, whereas GWS can be used to map the extent and severity of
175 hydrological drought. These experimental GRACE-based products are now incorporated into the
176 USDM and disseminated weekly via this website,
177 <http://drought.unl.edu/monitoringtools/nasagracedataassimilation.aspx>.

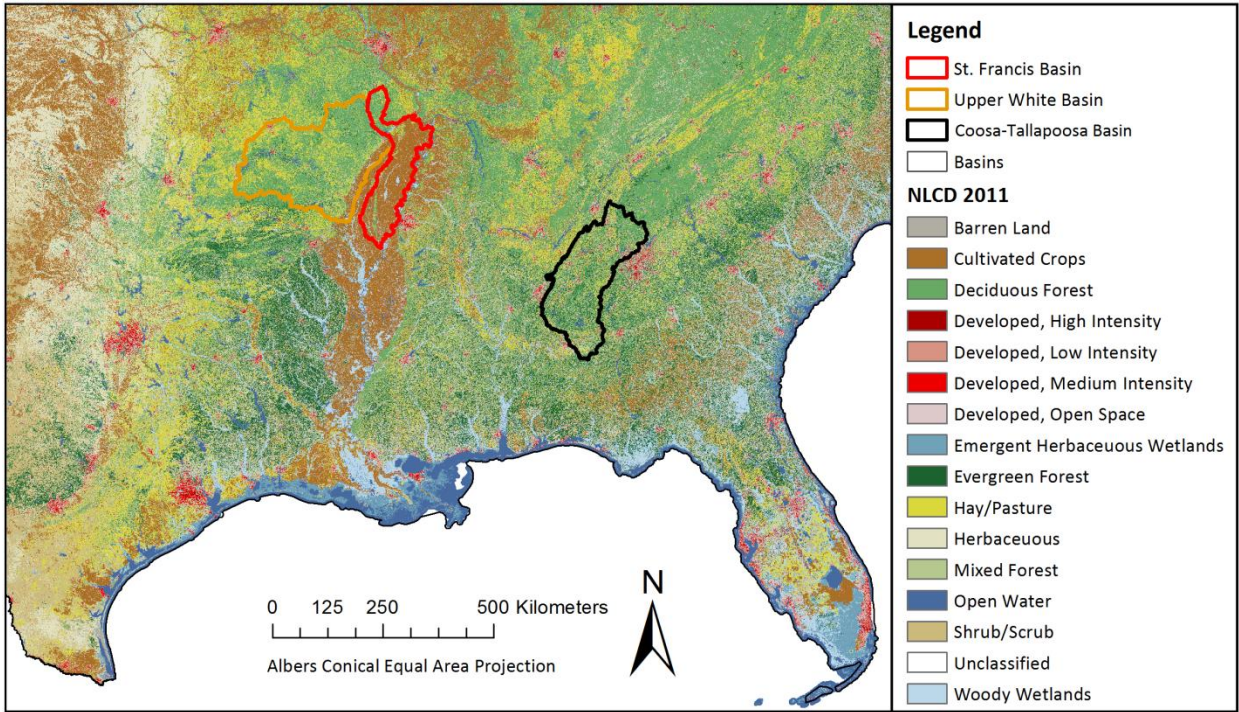
178 **2.7. Study area**

179 The study area is the southeastern U.S., where a humid warm temperate climate is prevalent
180 according to Köppen-Geiger climate classification (Kottek et al. 2006). The land cover is mainly
181 dominated by forests (mostly deciduous), cultivated crops and hay/pasture according to the
182 National Land Cover Database 2011 (NLCD 2011). Summers are characteristically hot and wet
183 with frequent thundershowers. Evaporative demand is high during summers, which makes the
184 region very susceptible to drought when seasonal rainfall is delayed.

185 Basins in the study area (Figures 1 and 2) were retrieved from the website of the Watershed
186 Boundary Dataset (WBD) (<http://nhd.usgs.gov/wbd.html>) to compare the drought indicators on
187 the basin-level. The WBD contains boundaries of drainage areas developed by the collaborative
188 effort among the US federal agencies in consistent with national federal standards, and

189 topographic and hydrologic features across the US and territories (U.S. Geological Survey and the
190 U.S. Department of Agriculture, Natural Resources Conservation Service 2013). Each basin in the
191 WBD is defined as the level-3 hydrological unit and assigned a unique identifier, hydrological unit
192 code (HUC). In this paper, we follow the naming conventions of hydrological units established in
193 the WBD, Region (Level-1), Basin (Level-3) and Watershed (Level-5), in the descending order with
194 respect to areal size.

195 Various crops such as corn, soybeans, rice, winter wheat, sorghum, cotton and peanuts are
196 grown in the study area, particularly in lower Mississippi region along Mississippi river (Figure 1).
197 During hot seasons, crops are irrigated to support crop growth and ensure high crop yields, and
198 irrigation is primarily concentrated over Lower Mississippi region (Figure 3) according to the
199 irrigation map, extracted from the MODIS Irrigated Agriculture Dataset for the US (MIrAD-US).
200 Pervez and Brown (2010) developed a geospatial model by combining remote sensing inputs such
201 as MODIS-NDVI and NLCD products with US Department of Agriculture (USDA) Census of
202 Agriculture irrigated area statistics to produce 2012 irrigated-agriculture areas dataset at 250-m
203 resolution.

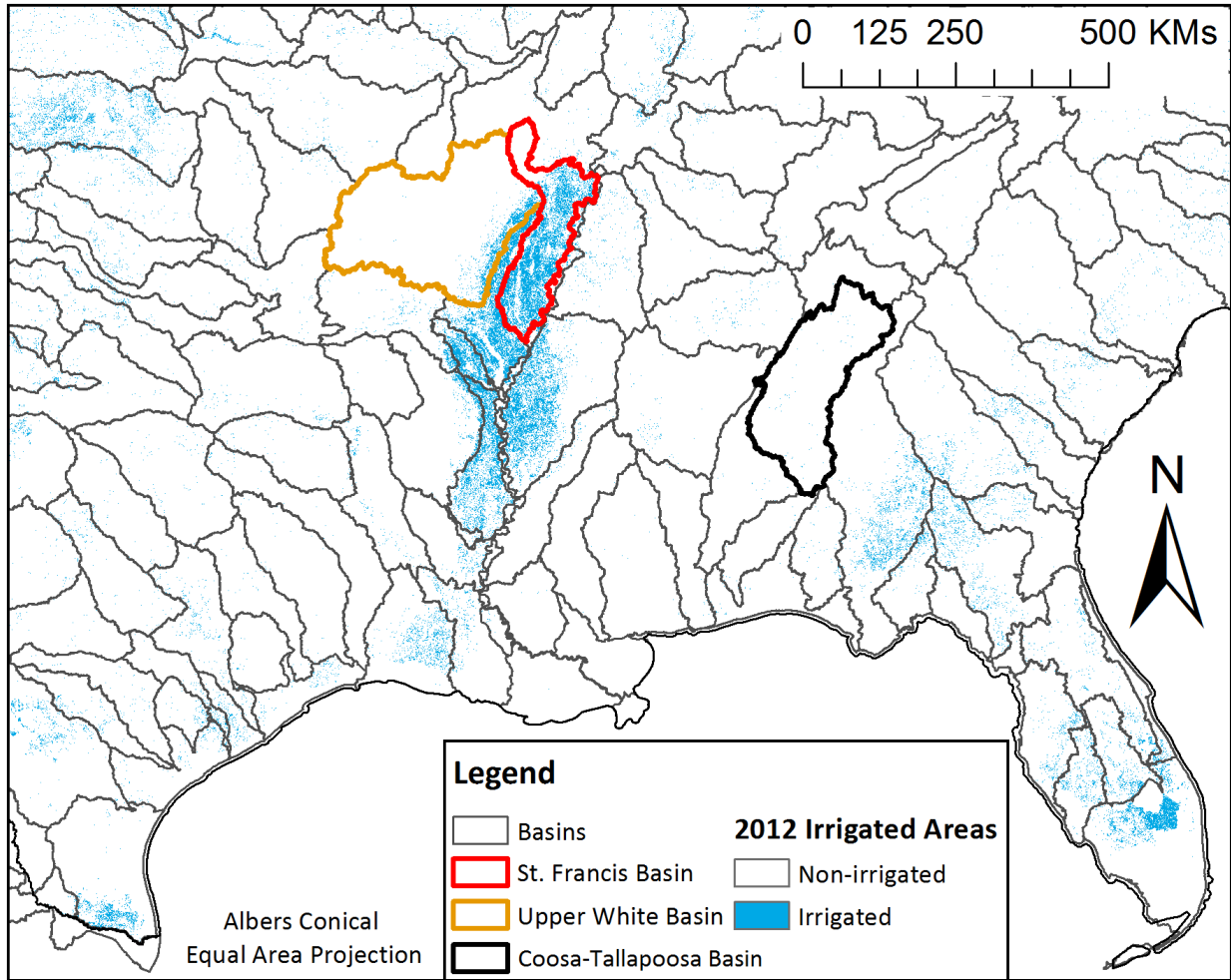


204

205

206

Figure 1 - Study area and boundaries of basins defined in the Watershed Boundaries Dataset (WBD). The background image is the land cover/land use subset from the National Land Cover Database 2011 (NLCD 2011).



207

208

209

Figure 2 - Irrigated areas in 2012 with respect to basins in the study area. Irrigation map is the subset of the MODIS-based Irrigated Areas Database (MirAD 2012)

210 3. Results

211 The spatial extent and severity of the 2012 drought are mapped by all drought indicators as

212 described in Section 2. The identical classification scheme (Table 1) is employed to identify

213 drought-affected regions and quantify severity of drought, ensuring that they are all in same

214 units. Therefore, percentile-based classification allows us to visually and quantitatively analyze

215 the drought results and draw meaningful conclusions. Visual comparison is necessary to analyze

216 the spatial extent of drought reported by all drought indicators, while quantitative examination

217 enables to inter-compare results with respect to drought onset, end and intensity. It is crucial to

218 re-emphasize that drought maps based on GWS percentiles is an indicator of hydrological
219 drought, while VCI-, TCI-, RTZSM- and SFSM-based drought maps provide agricultural drought
220 conditions. On the other hand, USDM-based drought maps collectively contain information about
221 hydrological, meteorological and agricultural drought.

222 **3.1. Spatial Representation of Drought**

223 GRACE- and MODIS-based maps are shown side-by-side in Figure 3 along with the USDM map
224 on August 6, 2012. These maps are valid for the week of 6-12 August, 2012, except that USDM
225 map is valid for the week of 7-13 August, 2012. Good correspondence between TCI- and VCI-
226 based maps was observed, although VCI indicated relatively large drought extent. Both maps
227 were also generally in good agreement with the USDM map and GRACE-SFSM, although they
228 displayed more extensive drought extent than MODIS-based drought indices. One stark
229 discrepancy among all indicators was seen in Georgia where both GRACE-derived indices and
230 USDM suggested severe-to-exceptional agricultural drought, while VCI and TCI did not indicate
231 any drought. Over Central US, drought extent reported by all indicators were in complete
232 agreement. Of all the indicators, the largest drought extent was reported by GRACE-GWS and -
233 RTZSM on August 6, 2012 (Figure 3).

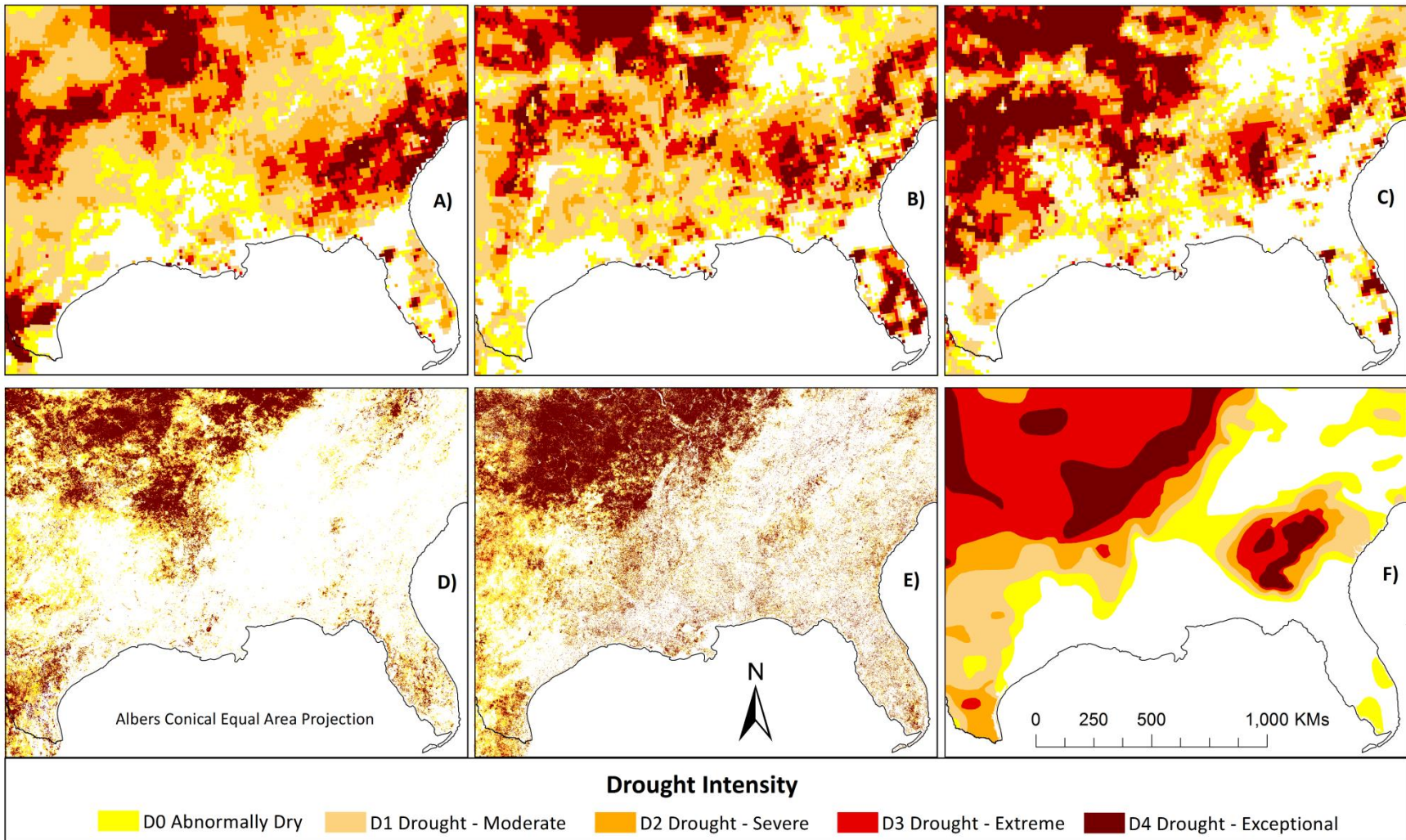
234 Another disagreement in indices was observed over Lower Mississippi region where the land
235 is cultivated for agricultural production. Crops in this region were irrigated in 2012 according to
236 irrigated agriculture map (Figure 2). Over this region, VCI did not report widespread reduced
237 vegetation activity (Figure 4), and TCI did not indicate elevated LST in comparison to other years,
238 both indicating a response of the respective index to the irrigation signal. On the other hand,

239 severe-to-exceptional drought was reported in the USDM and GRACE-derived SFSM over the St.
240 Francis basin (Figure 4), indicating that their broader-scale indices did not capture the local
241 irrigation practices that were taking place in 2012.

242 According to GRACE-based maps, ground water, root-zone and surface soil moisture all
243 deviated negatively from their historical averages throughout the study area, further signaling
244 both agricultural and hydrological drought throughout Southeast US. In Georgia where VCI and
245 TCI did not detect drought on August 6, 2012, both USDM and GRACE-based drought indicators
246 detected severe-to-exceptional drought. Over irrigated agriculture of Lower Mississippi region,
247 GRACE-based drought indicators were in agreement with USDM, but not with the MODIS-based
248 indicators (Figure 3 and 4). Disagreements between MODIS and GRACE indices were generally
249 situated along Appalachians Mountains (e.g., Blue Ridge mountains, and Ridge and Valley),
250 Piedmont Plateau and Atlantic Coastal Plains. Over these regions, GRACE drought indicators
251 reported severe-to-exceptional groundwater and soil moisture depletion in 2012. Drought
252 reported by GRACE-SFSM was not seen in VCI and TCI maps along Appalachians Mountains.
253 Broadly, discrepancies between GRACE-SFSM and MODIS indices seemed to be concentrated
254 over highly elevated areas along Appalachians Mountains (i.e., Blue Ridge Mountains).

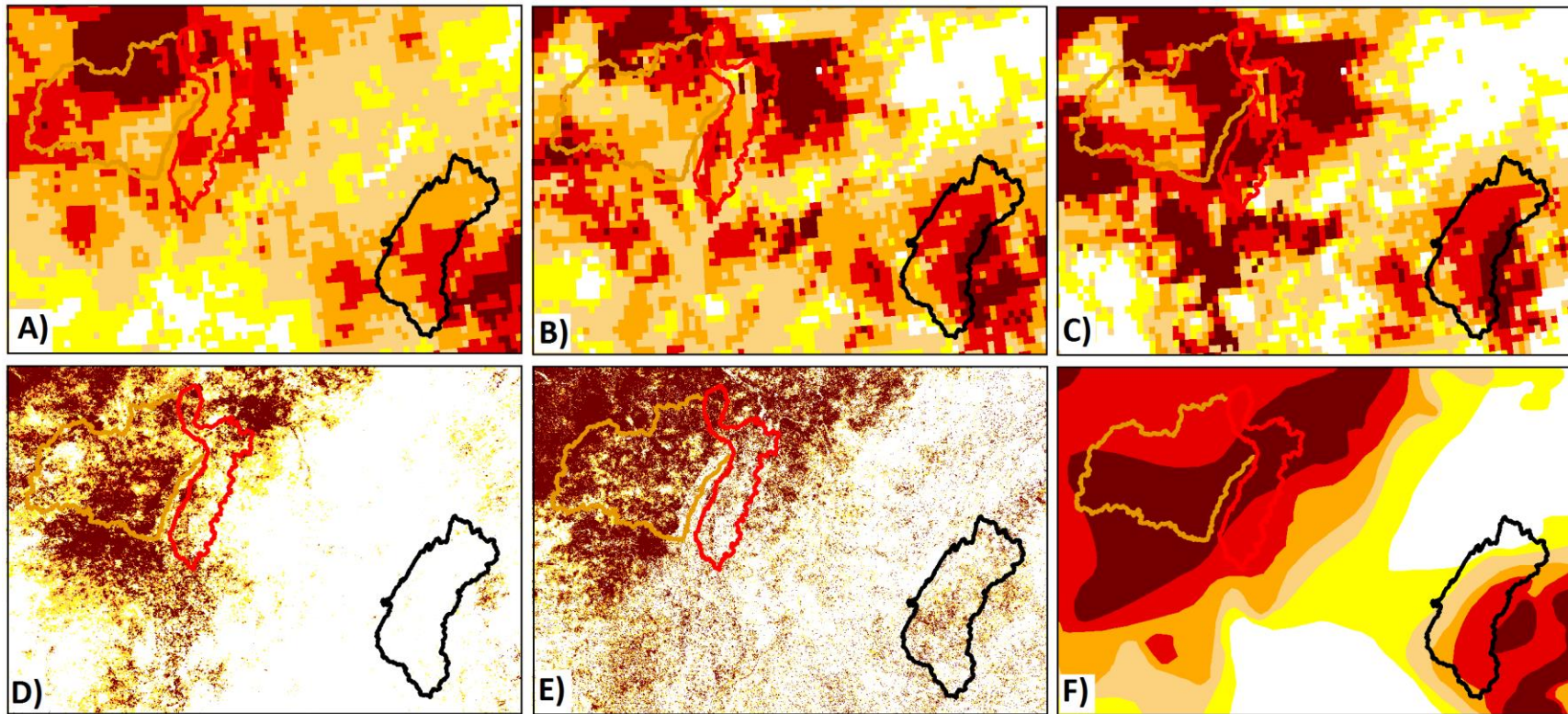
255 There is a well-known lagged response of vegetation (i.e., NDVI) to precipitation (Di,
256 Rundquist, and Han 1994), and Ji and Peters (2003) suggested 3-month lag of NDVI to
257 precipitation deficit. For this reason, 3-month Percent of Normal Precipitation for the time period
258 of June-August of 2012 (Figure 5) was retrieved from the NOAA's National Climatic Data Center
259 (NCDC) (<http://www.ncdc.noaa.gov/temp-and-precip/>). This precipitation deficit map broadly

260 matched drought extent indicated by VCI on August 6, 2012, while smaller drought extent was
261 reported by TCI. Both USDM and GRACE-SFSM indicated comparatively larger drought extent.



262
 263
 264
 265

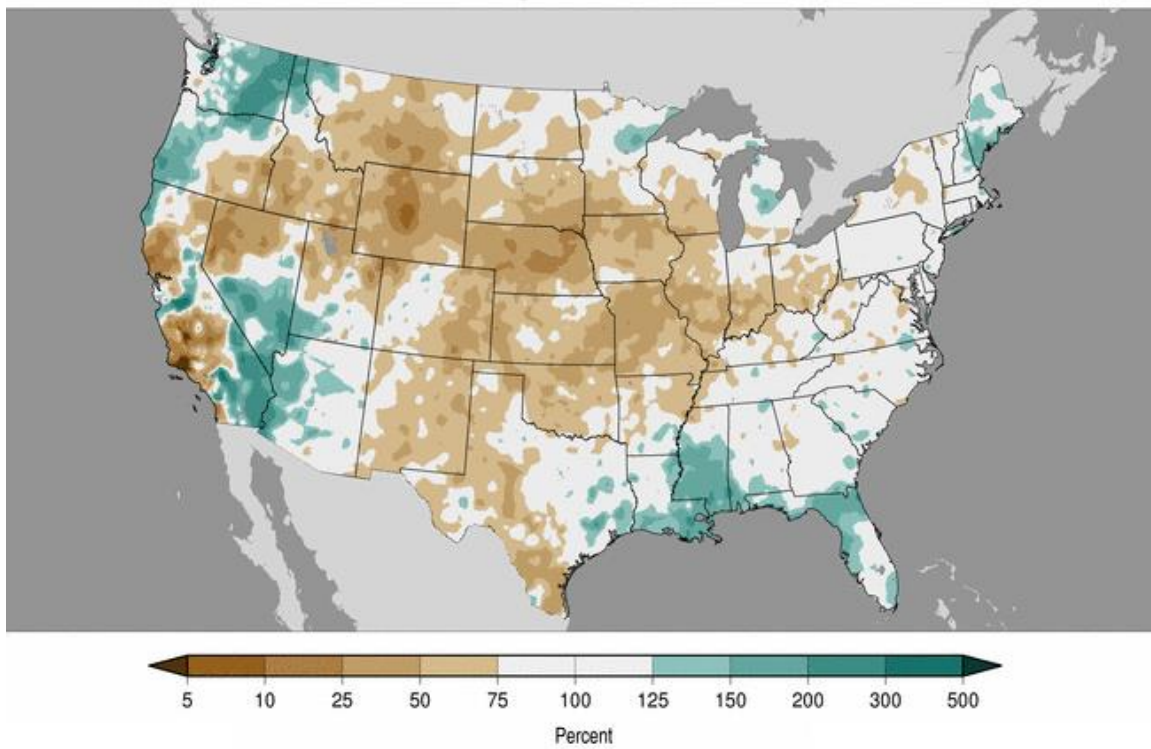
Figure 3 - GWS-based (A), RTZSM-based (B), SFSM-based (C), TCI-based (D), VCI-based (E) and USDM (F) drought maps. The USDM drought map is valid from August 7 to August 13, 2012, and all other maps are valid between August 6 and August 12, 2012.



267
268
269

Figure 4 - The close-up view of the drought maps over three basins on August 6, 2012 (USDM map is on August 7, 2012). Basin names are given in both Figures 1 and 2. The order of drought maps is same as the order in Figure 3.

Precipitation Percent of Average
June–August 2012
Average Period: 20th Century



270
271
272

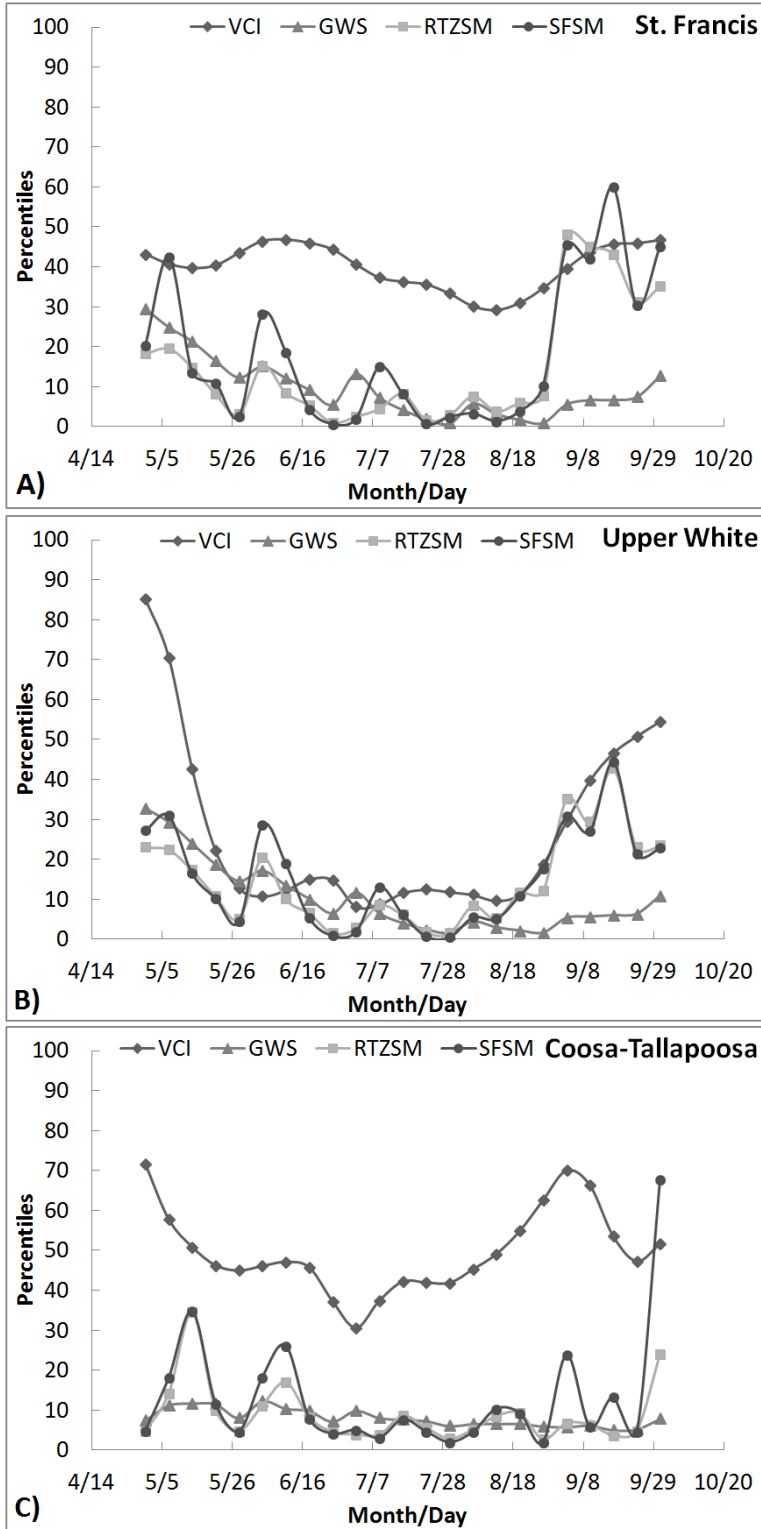
Figure 5 - 3-month Percent of Normal Precipitation for the time period of June- August, 2012 (NOAA-National Climatic Data Center 2012).

273 **3.2. Drought intensity**

274 Aside from analysis of spatial extent of drought, quantitative examination of drought intensity
275 is essential to reveal similarities and differences across indices. The comparison is conducted
276 based on the basin-level averages of drought indicators. The location of three basins in the study
277 area, Coosa-Tallapoosa (HUC6=031501), St. Francis (HUC6= 080202) and Upper White (HUC6=
278 110100) can be seen in both Figures 1 and 2. Coosa-Tallapoosa basin was selected for analysis
279 because MODIS-based drought indicators did not indicate any drought on August 6, 2012, in
280 contrast to USDM and GRACE-derived indicators (Figure 4). St. Francis basin was impacted by the
281 irrigation signal seen only in VCI and TCI, and all drought indicators were in good agreement in

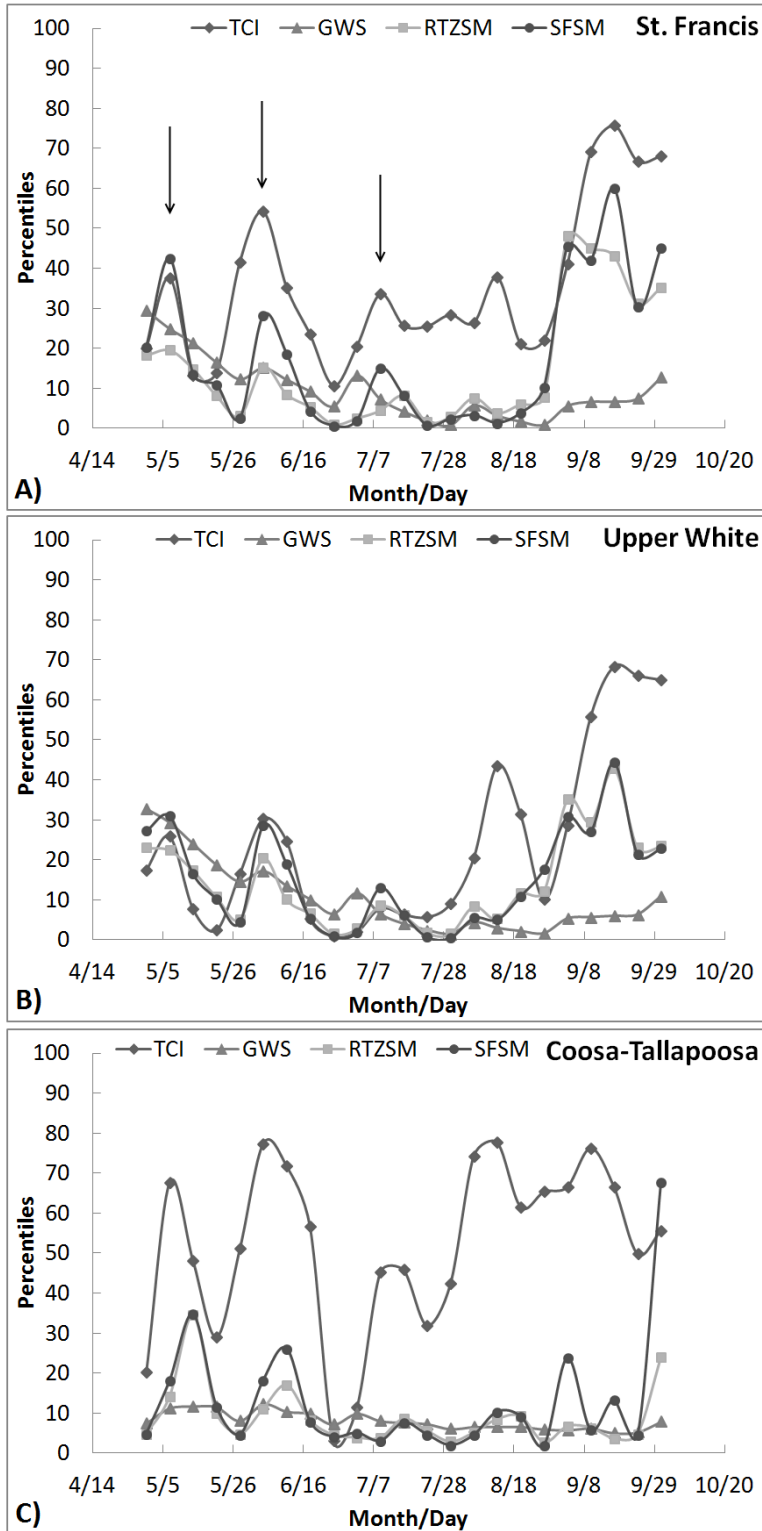
282 Upper White basin. Using basin boundaries, time series of VCI, TCI, RTZM, SFSM and GWS were
283 constructed between April 30, 2012 and October 1, 2012 on a weekly basis (Figures 6 and 7).

284 The results (Figure 6a) show that VCI was relatively constant above the drought threshold
285 (>30, Table 1) in St. Francis basin throughout 2012 where agriculture is irrigated (Figure 2).
286 Similarly, VCI didn't report any drought throughout the 2012 growing season in Coosa-Tallapoosa
287 basin where precipitation deficit was not seen between June and August of 2012 (Figure 5).
288 However, TCI fluctuated substantially around the drought threshold throughout 2012 in St.
289 Francis basin (Figure 7a) unlike Upper White (Figure 7b), indicating drought from May 14 to May
290 27, no drought from May 28 to June 17, drought from June 18 to July 8 and no drought from July
291 9 to July 15. Moreover, TCI was reported drought during the late June and early July of 2012
292 (Figure 7c) and at other times, no drought was indicated by TCI in Coosa-Tallapoosa basin. From
293 early June to late August in 2012, good correspondence was observed between all GRACE-based
294 and MODIS-based drought indicators in Upper White basin (Figure 6b and 7b), identifying
295 drought conditions. GRACE-derived indicators implied that all three basins experienced severe-
296 to-exceptional drought during the 2012 growing season.



297
 298
 299

Figure 6 - Basin averages of Vegetation Condition Index (VCI), Groundwater Storage (GWS), Root-Zone Soil Moisture (RTZSM) and Surface Soil Moisture (SFSM) in St. Francis (A), Upper White (B) and Coosa-Tallapoosa (C).



300
 301
 302

Figure 7 - Basin averages of Temperature Condition Index (TCI), Groundwater Storage (GWS), Root-Zone Soil Moisture (RTZSM) and Surface Soil Moisture (SFSM) in St. Francis (A), Upper White (B) and Coosa-Tallapoosa (C).

303 Correlation analysis was conducted using the time series of drought indicators in 2012. Each
304 time series is composed of 23 weekly observations spanning from April 30 to October 1, 2012.
305 The results revealed that TCI had higher statistically significant relationship at 0.01 significance
306 level with both SFSM and RTZSM than GWS in St. Francis and Upper White basins (Table 2). TCI
307 did not display any relation to groundwater variations in all basins. On the other hand, VCI
308 exhibited statistically significant relationship with GWS, RTZSM and SFSM only in Upper White
309 basin. Finally, there was no statistically significant correlation among any MODIS- and GRACE-
310 based indicators in Coosa-Tallapoosa basin.

311 Lagged response of NDVI and NDVI-based drought indices to soil moisture at various depths
312 up to 100cm was reported by other studies (Peng, Deng, and Di 2014; Adegoke and Carleton
313 2002) such that response of plants to soil moisture changes is not concurrent, rather exhibits
314 some time lag. Time lags up to 7 weeks are considered, and additional basin averages of GRACE-
315 derived GWS, RTZSM and SFSM are computed starting from January 16 until October 1, 2012,
316 ensuring that correlation coefficients are always computed from 23 weekly observations of all
317 drought indicators and the time period matches the growing season when vegetation is not
318 dormant (i.e., April 30 to October 1). The results (Table 3) show that correlations among drought
319 indicators improved considerably, thus suggesting that VCI exhibited lagged response to changes
320 in surface and root-zone soil moisture in St. Francis and Upper White basins. On the other hand,
321 no lag was found between TCI and GRACE-based RTZSM and SFSM, thus suggesting that LST
322 varies simultaneously with SFSM and RTZSM during dry years. Again, there was no significantly
323 lagged relationship among all indicators in Coosa-Tallapoosa basin. Overall, VCI lagged behind
324 RTZSM and SFSM about 2 weeks in St. Francis and Upper White basins. Therefore, TCI responded

325 to changes in SFSM and RTZSM more quicker than VCI in St. Francis and Upper White basins.
 326 Furthermore, the results pointed out that VCI and TCI had positive relationship in all basins, yet
 327 only statistically significant at 0.01 level in Upper White basin (Table 3). Time delay of 3 weeks
 328 between VCI and TCI was observed in Upper White basin.

329 **Table 2- Correlation coefficients (r) between VCI, TCI, SFSM, RTZSM and GWS in St. Francis, Upper White and**
 330 **Coosa-Tallapoosa basins. Time series are composed of observations time series between April 30 and October 1,**
 331 **2012. Statistically significant r at 0.01 significance level ($\alpha = 0.01$) are underlined. The critical r value is 0.53 at**
 332 **0.01 significance level.**

N=23	St. Francis		Upper White		Coosa-Tallapoosa	
r=0.53	VCI	TCI	VCI	TCI	VCI	TCI
GWS	0.46	-0.08	<u>0.64</u>	-0.13	-0.26	-0.08
RTZSM	0.43	<u>0.75</u>	<u>0.67</u>	<u>0.71</u>	0.07	0.17
SFSM	0.52	<u>0.78</u>	<u>0.67</u>	<u>0.64</u>	0.17	0.23
TCI	0.44		0.44		0.40	

333

334 **Table 3 - The lags and their correlation coefficients (r) between VCI, TCI, SFSM, RTZSM and GWS in St.**
 335 **Francis, Upper White and Coosa-Tallapoosa basins. Statistically significant r and lag at 0.01 significance level (α**
 336 **= 0.01) are underlined. The critical r value is 0.53 at 0.01 significance level.**

N=23	St. Francis				Upper White				Coosa-Tallapoosa			
r=0.53	VCI		TCI		VCI		TCI		VCI		TCI	
	lag	r	lag	r	lag	r	lag	r	lag	r	lag	r
GWS	0	0.46	0	-0.08	<u>0</u>	<u>0.64</u>	0	-0.13	7	0.14	0	-0.08
RTZSM	<u>2</u>	<u>0.55</u>	<u>0</u>	<u>0.75</u>	<u>2</u>	<u>0.87</u>	<u>0</u>	<u>0.71</u>	0	0.07	0	0.17
SFSM	<u>1</u>	<u>0.57</u>	<u>0</u>	<u>0.78</u>	<u>2</u>	<u>0.83</u>	<u>0</u>	<u>0.64</u>	0	0.17	0	0.23
TCI	1	0.46	-	-	<u>3</u>	<u>0.84</u>			1	0.50		

337 The correlation analysis among GRACE-derived SFSM, RTZSM and GWS revealed that SFSM
 338 was strongly correlated with RTZSM and GWS in all basins (Table 4), although relationship was
 339 relatively less strong in Coosa-Tallapoosa basin in 2012. SFSM relation to RTZSM was concurrent,
 340 while time lag of 4 weeks was observed between SFSM and GWS in all basins (Table 4). The results
 341 also suggested that there was a strong lagged-relationship between RTZSM and GWS in all basins,
 342 and the lag was 5 weeks in St. Francis and Upper White basin and 3 weeks in Coosa-Tallapoosa
 343 basin.

344 **Table 4 - The lags and their correlation coefficients (r) among GRACE-derived drought indicators in St.**
 345 **Francis, Upper White and Coosa-Tallapoosa basins. The critical r value is 0.46 at 0.01 significance level.**

N=31	SFSM					
r=0.46	St. Francis		Upper White		Coosa-Tallapoosa	
	lag	r	lag	r	lag	r
RTZSM	0	0.93	0	0.97	0	0.75
GWS	4	0.89	4	0.89	4	0.69
	RTZSM					
GWS	5	0.94	5	0.93	3	0.81

346 **4. Discussion**

347 Over irrigated agriculture in Lower Mississippi region, VCI did not report any drought although
 348 USDM clearly indicated drought in 2012. Especially in St. Francis basin, VCI provided more
 349 consistent results as opposed to TCI because LST responds more rapidly to prevailing weather
 350 conditions and irrigation events than NDVI. Furthermore, there was no discernible variation in
 351 SFSM, RTZSM and GWS unlike that observed in TCI over irrigated fields of St. Francis basin. It can
 352 be concluded that when agricultural fields were irrigated in 2012, LST decreased rapidly, and

353 subsequently TCI signaled no drought. When the surface became dry before the next irrigation
354 event, TCI reported drought after the sudden increase in LST (Figure 7a). In conclusion,
355 discrepancy between MODIS- and GRACE-based results in St. Francis can be easily explained by
356 irrigation, where irrigation is not considered in the decomposition of GRACE-based TWS into
357 SFSM, RTZSM and GWS (Houborg et al. 2012).

358 Correlation analysis revealed that the relationship between VCI and GRACE-based SFSM and
359 RTZSM is not concurrent, rather lagged in St. Francis and Upper White basins, whereas TCI had
360 concurrent positive relationships with both GRACE-derived SFSM and RTZSM. Approximately, VCI
361 exhibited 2-week lag to surface and root-zone soil moisture in 2012. Such conclusions with NDVI-
362 based indices were achieved by other studies (Peng, Deng, and Di 2014; Adegoke and Carleton
363 2002), as well. Correlations between VCI and other drought indicators were statistically
364 significant at 99% confidence level and improved considerably when lag effect is taken into
365 consideration in St. Francis and Upper White basins. However, the results of the correlation
366 analysis in St. Francis basin should be interpreted with caution since transfer of groundwater to
367 surface through irrigation and subsequently infiltration of that water down to root-zone is not
368 explicitly handled in CLSM. Besides, the land is heavily subject to anthropogenic effects (e.g.,
369 irrigation, harvesting of crops and farming practices) and timing of these events can vary
370 annually. Therefore, such drivers could be partly responsible for poorer correlation of VCI to
371 SFSM, RTZSM and TCI in St. Francis basin in comparison to Upper White basin. In Coosa-
372 Tallapoosa, no statistically significant relationship observed between VCI and TCI could be
373 attributed to frequent thundershowers, a common weather activity in summers across this
374 region. We demonstrated that TCI fluctuated substantially throughout the 2012 growing season

375 as opposed to VCI because LST responds wetting events (e.g., irrigation and thundershowers)
376 more quicker than NDVI.

377 We theorize that the timing of irrigation events can be detected by LST or TCI where LST
378 responds rapidly to irrigation event as sharp changes were seen in TCI time series in St. Francis
379 as opposed to Upper White basin. The methodology developed by Pervez and Brown (2010) only
380 decides whether or not a pixel is irrigated, but doesn't supply any information about the timing
381 of watering events. We suspect that sudden changes in the time series could be sign of irrigation
382 as depicted with arrows in Figure 6-A. However, LST products must be combined with MlrAD
383 irrigation dataset to eliminate likely errors because sharp fluctuations observed in Coosa-
384 Tallapoosa (Figure 7c) could lead to false-positives (i.e., Type I error). More research is needed to
385 validate our claim.

386 Utility of VCI to monitor meteorological drought was investigated by Quiring and Ganesh
387 (2010), however we demonstrated that although USDM indicated drought conditions (i.e.,
388 meteorological drought) over irrigated agriculture in Lower Mississippi region, drought was not
389 reported by VCI during the 2012 growing season (Figure 6-A). Therefore, VCI may not be a reliable
390 indicator of meteorological drought, but agricultural drought.

391 Our analysis of the 2012 drought in the Southeastern US demonstrated that the agreements
392 and disagreements over the extent and intensity of the 2012 drought exist among USDM, GRACE-
393 and MODIS-based drought indicators. We demonstrated that precipitation between June and
394 August (Figure 5) was at normal levels where disagreements between MODIS, GRACE and USDM
395 were seen over Georgia. Additionally, two principal factors, irrigation and lagged response of
396 vegetation to variations in soil moisture, could be partially responsible for these disagreements.

397 Another factor that may contribute to these disagreements is the type of drought reported by
398 these indicators such that GRACE-GWS is a measure of hydrological drought indicator, while the
399 rest could be more suitable in depicting agricultural drought conditions.

400 **5. Conclusions**

401 USDM, GRACE- and MODIS-based drought maps were successful in depicting the drought of
402 2012 despite disagreements over its extent and intensity, and they all indicated that Southeast
403 US experienced severe-to-exceptional drought in 2012. Both MODIS-based and GRACE-SFSM
404 drought maps closely mimicked the surface conditions depicted in the USDM maps except over
405 irrigated areas, Georgia and along Appalachians Mountains (e.g., Blue Ridge mountains, and
406 Ridge and Valley). However, short-term precipitation deficit map agreed with MODIS indices in
407 these regions, indicating normal precipitation conditions compared to long-term average
408 conditions. GRACE-based GWS implied that majority of the southeastern US experienced
409 moderate-to-extreme hydrological drought, thus suggesting that groundwater sources severely
410 depleted during the drought of 2012. We demonstrated that disagreements over the extent and
411 intensity of the 2012 drought across all drought indicators could result from irrigation, complex
412 lagged response of vegetation to precipitation and soil moisture and the type of drought these
413 indicators report (e.g., meteorological, agricultural and hydrological drought).

414 **Acknowledgments**

415 This research was supported by an appointment to the NASA Postdoctoral Program at the
416 Goddard Space Flight Center (GSFC), administered by Universities Space Research Association
417 (USRA) through a contract with NASA.

- 419 Adegoke, Jimmy O., and Andrew M. Carleton. 2002. "Relations between Soil Moisture and
420 Satellite Vegetation Indices in the U.S. Corn Belt." *Journal of Hydrometeorology* 3 (4):
421 395–405. doi:10.1175/1525-7541(2002)003<0395:RBSMAS>2.0.CO;2.
- 422 Anderson, Martha C., and William Kustas. 2008. "Thermal Remote Sensing of Drought and
423 Evapotranspiration." *Eos, Transactions American Geophysical Union* 89 (26): 233.
424 doi:10.1029/2008EO260001.
- 425 Brown, Jesslyn F., Brian Wardlow, T. Tadesse, Michael J. Hayes, and Bradley C. Reed. 2008. "The
426 Vegetation Drought Response Index (VegDRI): A New Integrated Approach for Monitoring
427 Drought Stress in Vegetation." *GIScience & Remote Sensing* 45 (1): 16–46.
428 doi:10.2747/1548-1603.45.1.16.
- 429 Deng, Meixia, Liping Di, Weiguo Han, Ali Levent Yagci, Chunming Peng, and Gil Heo. 2013. "Web-
430 Service-Based Monitoring and Analysis of Global Agricultural Drought." *Photogrammetric*
431 *Engineering & Remote Sensing* 79 (10): 929–943. doi:10.14358/PERS.79.10.929.
- 432 Di, Liping, D. C. Rundquist, and Luoheng Han. 1994. "Modelling Relationships between NDVI and
433 Precipitation during Vegetative Growth Cycles." *International Journal of Remote Sensing*
434 15 (10): 2121–2136. doi:10.1080/01431169408954231.
- 435 Houborg, Rasmus, Matthew Rodell, Bailing Li, Rolf Reichle, and Benjamin F. Zaitchik. 2012.
436 "Drought Indicators Based on Model-Assimilated Gravity Recovery and Climate
437 Experiment (GRACE) Terrestrial Water Storage Observations." *Water Resources Research*
438 48 (7): W07525. doi:10.1029/2011WR011291.
- 439 Huete, A. R., K Didan, T Miura, E.P. Rodriguez, X Gao, and L.G. Ferreira. 2002. "Overview of the
440 Radiometric and Biophysical Performance of the MODIS Vegetation Indices." *Remote*
441 *Sensing of Environment* 83 (1-2): 195–213. doi:10.1016/S0034-4257(02)00096-2.
- 442 Ji, L., and A. J. Peters. 2003. "Assessing Vegetation Response to Drought in the Northern Great
443 Plains Using Vegetation and Drought Indices." *Remote Sensing of Environment* 87 (1): 85–
444 98. doi:10.1016/S0034-4257(03)00174-3.
- 445 Kogan, F. 1997. "Global Drought Watch from Space." *Bulletin of the American Meteorological*
446 *Society* 78 (4): 621–636. doi:10.1175/1520-0477(1997)078<0621:GDWFS>2.0.CO;2.
- 447 Kogan, F. 2001. "Operational Space Technology for Global Vegetation Assessment." *Bulletin of*
448 *the American Meteorological Society* 82 (9): 1949–1964. doi:10.1175/1520-
449 0477(2001)082<1949:OSTFGV>2.3.CO;2.
- 450 Koster, Randal D., Max J. Suarez, Agnès Ducharne, Marc Stieglitz, and Praveen Kumar. 2000. "A
451 Catchment-Based Approach to Modeling Land Surface Processes in a General Circulation
452 Model: 1. Model Structure." *Journal of Geophysical Research: Atmospheres* 105 (D20):
453 24809–24822. doi:10.1029/2000JD900327.

- 454 Kottek, Markus, Jürgen Grieser, Christoph Beck, Bruno Rudolf, and Franz Rubel. 2006. "World
455 Map of the Köppen-Geiger Climate Classification Updated." *Meteorologische Zeitschrift*
456 15 (3): 259–263. doi:10.1127/0941-2948/2006/0130.
- 457 NOAA-National Climatic Data Center. 2012. "3-Month Percent of Normal Precipitation." *National*
458 *Temperature and Precipitation Maps*. [http://www.ncdc.noaa.gov/monitoring-](http://www.ncdc.noaa.gov/monitoring-content/sotc/national/grid-prcp/prcp-pon-201206-201208.gif)
459 [content/sotc/national/grid-prcp/prcp-pon-201206-201208.gif](http://www.ncdc.noaa.gov/monitoring-content/sotc/national/grid-prcp/prcp-pon-201206-201208.gif).
- 460 Peng, Chunming, Meixia Deng, and Liping Di. 2014. "Relationships Between Remote-Sensing-
461 Based Agricultural Drought Indicators and Root Zone Soil Moisture: A Comparative Study
462 of Iowa." *IEEE Journal of Selected Topics in Applied Earth Observations and Remote*
463 *Sensing* 7 (11): 4572–4580. doi:10.1109/JSTARS.2014.2344115.
- 464 Pervez, Md Shahriar, and Jesslyn F. Brown. 2010. "Mapping Irrigated Lands at 250-M Scale by
465 Merging MODIS Data and National Agricultural Statistics." *Remote Sensing* 2 (10): 2388–
466 2412. doi:10.3390/rs2102388.
- 467 Quiring, Steven M., and Srinivasan Ganesh. 2010. "Evaluating the Utility of the Vegetation
468 Condition Index (VCI) for Monitoring Meteorological Drought in Texas." *Agricultural and*
469 *Forest Meteorology* 150 (3): 330–339. doi:10.1016/j.agrformet.2009.11.015.
- 470 Rippey, Bradley R. 2015. "The U.S. Drought of 2012." *Weather and Climate Extremes*, USDA
471 Research and Programs on Extreme Events, 10, Part A (December): 57–64.
472 doi:10.1016/j.wace.2015.10.004.
- 473 Rodell, Matthew. 2012. "Satellite Gravimetry Applied to Drought Monitoring." In *Remote Sensing*
474 *of Drought*, 261–278. Drought and Water Crises. CRC Press.
475 <http://www.crcnetbase.com.mutex.gmu.edu/doi/abs/10.1201/b11863-15>.
- 476 Rodell, Matthew, and J. S. Famiglietti. 1999. "Detectability of Variations in Continental Water
477 Storage from Satellite Observations of the Time Dependent Gravity Field." *Water*
478 *Resources Research* 35 (9): 2705–2723. doi:10.1029/1999WR900141.
- 479 Solano, Ramon, Kamel Didan, Andree Jacobson, and A. R. Huete. 2010. *MODIS Vegetation Index*
480 *(MOD13) C5 User's Guide Version 2*. Vegetation Index and Phenology Lab, The University
481 of Arizona.
482 http://vip.arizona.edu/documents/MODIS/MODIS_VI_UsersGuide_01_2012.pdf.
- 483 Svoboda, Mark, Doug Lecomte, Mike Hayes, Richard Heim, Karin Gleason, Jim Angel, Brad Rippey,
484 et al. 2002. "The Drought Monitor." *Bulletin of the American Meteorological Society* 83
485 (8): 1181–1190. doi:10.1175/1520-0477(2002)083<1181:TDM>2.3.CO;2.
- 486 Swain, Sharmistha, Brian D. Wardlow, Sunil Narumalani, T. Tadesse, and Karin Callahan. 2011.
487 "Assessment of Vegetation Response to Drought in Nebraska Using Terra-MODIS Land
488 Surface Temperature and Normalized Difference Vegetation Index." *GIScience & Remote*
489 *Sensing* 48 (3): 432–455. doi:10.2747/1548-1603.48.3.432.
- 490 Swenson, Sean, Pat J.-F. Yeh, John Wahr, and James Famiglietti. 2006. "A Comparison of
491 Terrestrial Water Storage Variations from GRACE with in Situ Measurements from
492 Illinois." *Geophysical Research Letters* 33 (16): L16401. doi:10.1029/2006GL026962.

493 Tadesse, T., J Brown, and M Hayes. 2005. "A New Approach for Predicting Drought-Related
494 Vegetation Stress: Integrating Satellite, Climate, and Biophysical Data over the U.S.
495 Central Plains." *ISPRS Journal of Photogrammetry and Remote Sensing* 59 (4): 244–253.
496 doi:10.1016/j.isprsjprs.2005.02.003.

497 Tapley, B. D., S. Bettadpur, M. Watkins, and C. Reigber. 2004. "The Gravity Recovery and Climate
498 Experiment: Mission Overview and Early Results." *Geophysical Research Letters* 31 (9):
499 L09607. doi:10.1029/2004GL019920.

500 The National Drought Mitigation Center. 2016. "U.S. Drought Monitor Classification Scheme."
501 *United States Drought Monitor*.
502 <http://droughtmonitor.unl.edu/AboutUs/ClassificationScheme.aspx>.

503 Tucker, C. J., and Bhaskar J. Choudhury. 1987. "Satellite Remote Sensing of Drought Conditions."
504 *Remote Sensing of Environment* 23 (2): 243–251. doi:10.1016/0034-4257(87)90040-X.

505 U.S. Geological Survey and the U.S. Department of Agriculture, Natural Resources Conservation
506 Service. 2013. "Techniques and Methods 11–A3." In *Federal Standards and Procedures*
507 *for the National Watershed Boundary Dataset (WBD)*, 4th ed., 63. Reston, VA: U.S.
508 Geological Survey and the U.S. Department of Agriculture, Natural Resources
509 Conservation Service. <http://pubs.usgs.gov/tm/11/a3/>.

510 Wahr, John, Sean Swenson, Victor Zlotnicki, and Isabella Velicogna. 2004. "Time-Variable Gravity
511 from GRACE: First Results." *Geophysical Research Letters* 31 (11): L11501.
512 doi:10.1029/2004GL019779.

513 Wan, Zhengming. 2007. *Collection-5 MODIS Land Surface Temperature Products Users' Guide*.
514 ICES, University of California, Santa Barbara.
515 [http://www.ices.ucsb.edu/modis/LstUsrGuide/MODIS_LST_products_Users_guide_C5.](http://www.ices.ucsb.edu/modis/LstUsrGuide/MODIS_LST_products_Users_guide_C5.pdf)
516 pdf.

517 Wilhite, Donald A. 2000. "Drought as a Natural Hazard: Concepts and Definitions." In *Drought: A*
518 *Global Assessment*, edited by Donald A. Wilhite, 1st ed., 3–18. Hazards and Disasters.
519 London: Routledge.

520 Yagci, Ali Levent, Liping Di, Meixia Deng, Weiguo Han, and Chunming Peng. 2011. "Agricultural
521 Drought Monitoring From Space Using Freely Available MODIS Data." In *Proceedings of*
522 *18th William T. Pecora Memorial Remote Sensing Symposium*. Herndon, VA: ASPRS.

523 Yagci, Ali Levent, Liping Di, Meixia Deng, Genong Yu, and Chunming Peng. 2012. "Global
524 Agricultural Drought Mapping: Results for the Year 2011." In *2012 IEEE International*
525 *Geoscience and Remote Sensing Symposium*, 3764–3767. Munich, Germany: IEEE.
526 doi:10.1109/IGARSS.2012.6350498.

527 Zaitchik, Benjamin F., Matthew Rodell, and Rolf H. Reichle. 2008. "Assimilation of GRACE
528 Terrestrial Water Storage Data into a Land Surface Model: Results for the Mississippi River
529 Basin." *Journal of Hydrometeorology* 9 (3): 535–548. doi:10.1175/2007JHM951.1.

530